

Thermoelectrical Modelling of the Effect of Metal Height and Cathode Erosion on Cell Heat Balance

Simon-Olivier Tremblay¹, Daniel Marceau², Antoine Godefroy³, Sébastien Charest⁴
and Jules Côté⁵

1. Research Professional

2. Professor

Centre universitaire de recherche sur l'aluminium (CURAL) – Regroupement stratégique sur l'aluminium (REGAL) – Université du Québec à Chicoutimi, Saguenay, Canada

3. Supervisor Dev-Tech Electrolysis Process

4. Senior Director Engineering, Information Technology and Automation

5. Vice President Major Projects

Aluminerie Alouette, Sept-Îles, Canada

Corresponding author: simon_olivier1@hotmail.com

<https://doi.org/10.71659/icsoba2024-al055>

Abstract

The adaptation of the control strategy to be used during the life of the aluminium reduction cell is a critical issue. The evolution of the dynamic behaviour of the cell leads to significant changes in the thermal balance and current efficiency, which require such adaptation to maintain an efficient process. To do so, a good understanding of the parameters affecting the cell behaviour is required. One of those parameters is the metal mass in the cell which affects, among others, the thermal balance and hence the protective ledge. During its life, the erosion of the cathode leads to an additional mass of metal in the cell, which may also change this equilibrium. To guide the control strategy, a calibrated thermoelectrical quarter-cell model (ANSYS™) is used to investigate the effect of the metal mass via the variation of the metal pad height and/or the eroded cathode profile. The results obtained from the simulations allow to estimate the energy input correction for a given metal mass in order to assure proper protective ledge/thermal balance. This estimation is based on the minimisation of the change in the ledge profile between a specific scenario and the reference one as obtained with the calibrated conditions. Such procedure and results give critical information for further optimisation of the operational procedure.

Keywords: Aluminium reduction cell, Metal height, Thermal balance, Cell thermoelectrical modelling.

1. Introduction

The dynamic behavior of the cell results in continuous changes of the cell state due to the nature of the process and the required interventions such as: metal tapping, cathode erosion, anode change, evolution of material properties, bath chemistry evolution, anode effects and many others. Some of those elements such as the metal tapping and the cathode erosion phenomena can lead to operating the reduction cell with a higher mass of metal mainly because of three reasons:

- Unforeseen events in the plant cause the delay of the planification which includes the tapping procedure of the metal leading to higher metal pad height for some reduction cells
- Unavoidable and continuous erosion of the cathodes/lining leading to an additional mass of metal for a same metal pad height
- Change in the target value of the metal pad height in order to adjust the ledge thickness toward the optimal

In the aluminum industry, it is well known that operating at a higher metal pad height change the thermal balance leading, for instance, to an increase of the heat loss by the sides of the cell and

then a thicker protective ledge. Therefore, when operating with an additional mass of metal, it is necessary to take the right action to remain with an optimal thermal balance. Amongst others, one of the available actions is to change the internal heat of the cell via the cell voltage/ACD. In order to determine the amplitude of this correction, this paper will focus on the effect of the mass of metal on the thermal behaviour of the reduction cell.

2. Problem Statement and Objective

Operating with a different mass of metal causes a variation in the thermal balance of the cell, more specifically to the:

- Protective ledge thickness
- Location of the critical isotherm in the lining
 - o 955 °C, bath liquidus
 - o 820 °C, harmful for insulating lining
 - o 660 °C, metal liquidus
- Heat loss distribution around the cell

However, since the behavior of the cell is highly transient and complex, it is difficult to properly quantify the correction to be made to the cell voltage to maintain an adequate thermal balance for a given additional metal mass. Also, there is no guarantee that a correction in the cell voltage leading to an adequate protective ledge (for instance) will also lead to critical isotherm in the lining that are harmful for the operation and cell life. Which brings us to the objectives:

- Determine the effect of an increase of the metal pad height on the thermal behavior
- Determine the effect of an increase of the cathode erosion on the thermal behavior
- For a given additional mass of metal, determine the cell voltage correction in order to:
 - o return to the optimal ledge thickness
 - o ensure that the critical isotherms (955 °C, 820 °C, 660 °C) are not harmful to the operation and the cell life

3. Proposed Approach

The proposed approach consists on the utilization of a transient $\frac{1}{4}$ reduction cell model using 3D finite element method in order to evaluate the thermal and electrical behavior of a reduction cell for the following scenarios:

1. Normal metal pad height (15 cm) without cathode erosion (reference scenario)
2. Additional metal pad height (22 cm) without cathode erosion
3. Normal metal pad height (15 cm) with an estimated 5-year cathode erosion

To represent the cell thermal and electrical behavior properly, the model must include the proper geometry, material properties and boundary conditions. All those elements were determined and calibrated previously, as explained in detail in [1].

Regarding the ledge profile, it is required that the ledge hot surface (corresponding to the 955 °C isotherm) be positioned according to the TE behavior of the reduction cell. To do so, the strategy is to create a fictive material for the volume that include the liquids (metal/bath) and the solid ledge. The properties of this selected volume are those of the liquid metal/bath above 955 °C and those of the solid ledge below 955 °C. This element will be discussed further in the model description.

The model is then used to predict a resulting ledge profile for each one of the scenarios (1 to 3). An external calculation procedure is then used to quantitatively compare the changes in the ledge profile between the scenario under investigation and the reference scenario. Finally, simulations of the scenarios with additional metal (2–3) will be carried out in order to estimate the additional

internal energy (via the increase of the cell voltage) necessary to return, as close as possible, to the reference ledge profile. This value will therefore allow the industry to know more accurately the correction to be applied on the cell voltage (for a given additional metal mass) in order to maintain an adequate ledge profile as well as to validate the location of the critical isotherms in the lining.

4. The Finite Element Model

The first goal is to develop a model that accurately represent the reduction cell during the steady state. To do so, the model was calibrated using thermal and electrical data during a measurement campaign carried out at Aluminerie Alouette Inc. (AAI) following a specific instrumentation plan (as explained in detail in [1]). A cell age of 152 days was selected for the calibration in steady state considering the following elements at that specific time:

- Good operation stability
- Normal and stable internal heat
- Minimal cathode erosion
- No more additional cell resistance
- Minimal change in thermal and electrical lining properties (due to vitrification of the lining for instance)
- Available cover thickness measurement
- Available ledge profile measurement
- Available bath temperature and superheat

4.1 Geometry

Considering the double geometrical symmetry of the reduction cell, only the quarter of the cell is considered by using the representative boundary conditions. Figure 1 shows the different components of the cell which represent the reference scenario during the steady state operation.

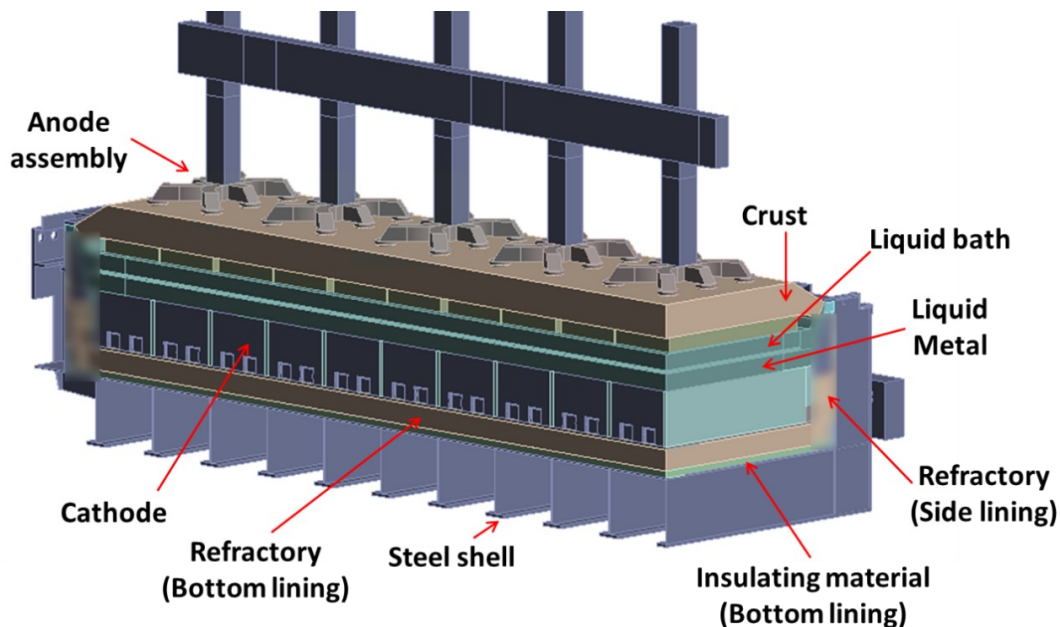


Figure 1. Discrete representation of the reduction cell during steady state.

The green region on Figure 2 shows specifically where the ledge surface can be potentially located. As we can see, there is no definition of the ledge surface since it will be computed by the

model and corresponding to the 955 °C isotherm. To do so, a fictive multiphasic material is used for each of these volumes with the following conditions:

1. Liquid bath/Solid ledge: material properties of the liquid bath over 955 °C and of the solid ledge under 955 °C.
2. Liquid metal/Solid ledge: material properties of the liquid metal over 955 °C and of the solid ledge under 955 °C.

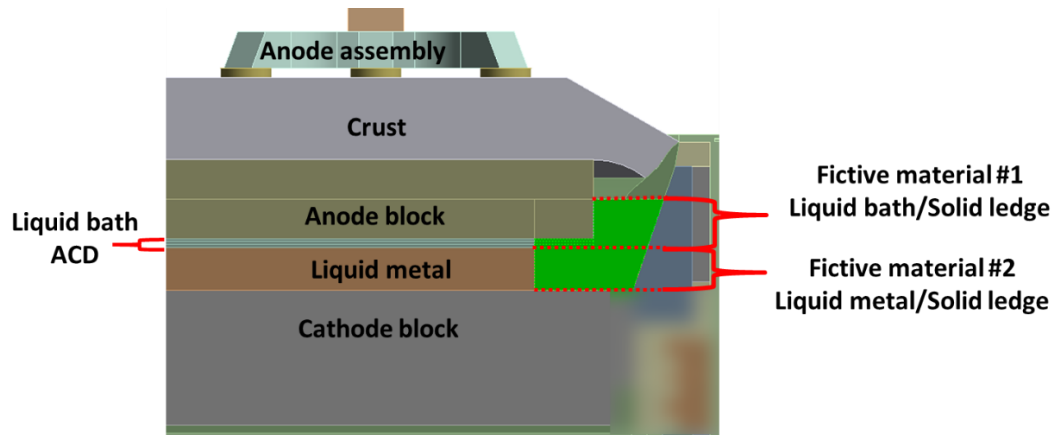


Figure 2. Region associated to the fictive multiphasic materials.

4.1.1 Computation of the Erosion Profiles

Computation of the erosion profiles has been done using numerous data obtained during autopsy on a reduction cell as well as the inventory of metal mass in the cells during their lifespan. Figure 3(a) shows the collection of data used in this investigation as well as the proposed 8th degree polynomial fitting. Considering a hypothetical symmetry of the erosion, the data have been reduced on half width of the cell to enrich the approximation. Considering the age of the autopsied cell (\check{t}), the function has been calibrated to show the observed average annual maximum erosion at a specific location such as:

$$p(x, t) = \frac{t}{\check{t}} \sum_{i=0}^8 a_i \cdot x^i \quad (1)$$

where:

- x Position along the short side
- a_i Given in Table 1
- t Time

Table 1. Coefficient a_i of the 8th degree polynomial approximation.

a_0	a_1	a_2	a_3	a_4	a_5	a_6	a_7	a_8
-0.04	0.14	-6.25	38.54	-106.08	155.14	-124.86	52.09	-8.78

Expression (1) assume a linear evolution of the erosion over time which have been confirmed after many autopsies carried out on reduction cells of different ages at AAI. Figure 3(b) shows the evolution of the erosion profile during five years of operation.

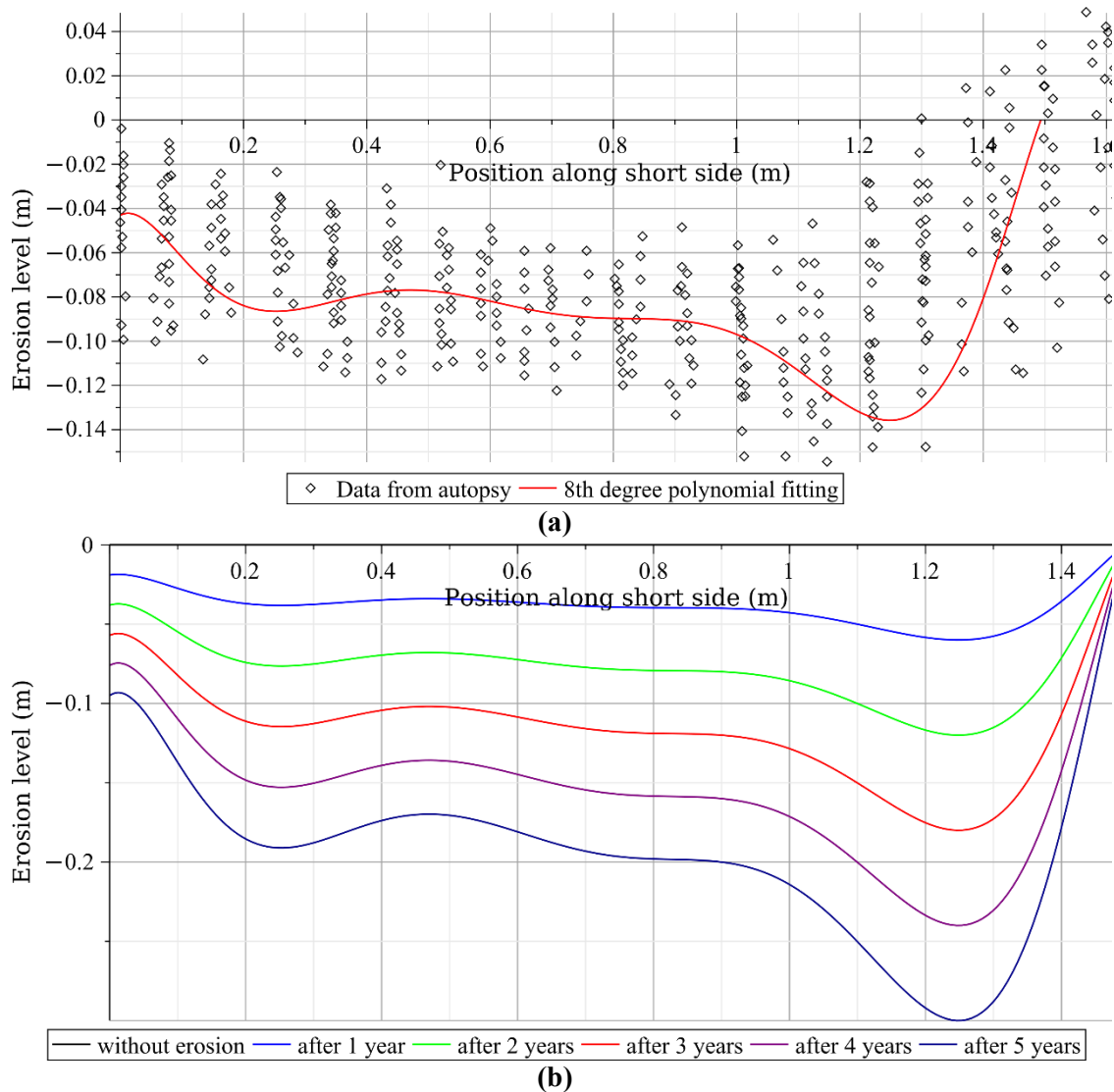


Figure 3. Estimation of the erosion profile on industrial data (a). Evolution of the erosion profile with time (b).

To obtain the full profile, a periodical evolution is built along the long side using trigonometric function such as:

$$p(y) = a \cdot \cos(b(y - h)) + k \quad (2)$$

where a, b, h, k have been calibrated to fit the observed total mass of metal in the reduction cell at the age of the cell under investigation and the observed ratio of erosion of about 12% between the mid width of the cathode and the small joint of ramming paste. The final expression is obtained by combining (1) and (2) such as:

$$p(x, y, t) = p(x, t) \cdot p(y) \quad (3)$$

For a given age (t), Expression (3) is used to determine the erosion profile which is then imported in ANSYS™ to modify the cathode surface. Figure 4 shows the resulting erosion profile after five years of operation in the geometry.

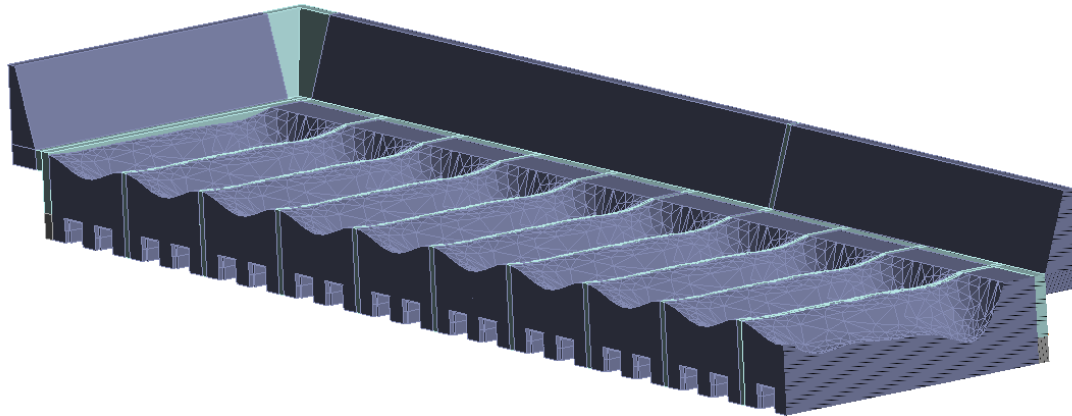


Figure 4. Resulting representation of the cathode surface profile in the geometry.

4.2 Analysis Type and Boundary Conditions

A transient TE analysis is used in order to represent the evolution of the ledge (955 °C isotherm in the dedicated volumes) until equilibrium is reached. The transient simulation is required since the fictive multiphasic materials (liquids/ledge) includes abrupt variation of the thermal conductivity and electrical resistivity near 955 °C. Following the chosen approach, this abrupt variation is explained by the transition between the solid ledge and the liquids properties. This way, the time stepping strategy is selected in order to minimise numerical instability and achieved convergence until the steady state is achieved.

Tables 2 shows the boundary conditions used for the TE analysis:

Table 2. Boundary conditions of the model.

Current at the connection surface between the positive risers and the anode beam (400 kA / cell)	100 kA
Voltage on the lower surface of the bus bar	0 V
Ambient temperature at the exterior of the cell (based on AAI measurements)	37 °C
Ambient temperature inside the cell (based on AAI measurements)	140 °C
Convection coefficient on surfaces as calibrated previously (based on AAI measurements)	- Inside the cell: 14 W/m ² ·K - Outside the cell: 9.5 W/m ² ·K
Electrical contact resistance (ECR) at the cast iron to carbon interface (from [1, 2])	0.5 Ω·mm ²

Also, since the model does not represent the heat transfer cause by the movement of the liquids (which is non-negligible), it is necessary to use an effective thermal conductivity. Based on [3, 4], the effective thermal conductivity of the liquid metal pad was estimated to be around 20 times its motionless thermal conductivity. As for the calibration of the model, the only remaining parameter to be calibrated is the ohmic resistance coming from the ACD which is responsible for the internal heat in the cell. The ACD in the model needs to include the ohmic resistance from the bath (with an unknown measured ACD) and from the bubbles. Then, considering a fix fictive ACD of 30 mm in the model (for meshing quality reasons), the electrical resistivity of the liquid bath was used as a fudging factor of the ohmic resistance in order to accurately represent the right amount of internal heat generated in the reduction cell. This calibration was validated using the *in-situ* measurements of the temperature distribution from [1, 2], the cell voltage and the ledge profile/thickness.

It should be noted that the chosen numerical approach does not consider the changes in the volume, chemical composition and bath properties which are associated with a variation of the thermal balance in reality (hence a metal mass variation).

5. Computation of the Ledge Profile

For each scenario (metal pad height and erosion time), the sub-mesh dedicated to the potential metal/bath phase change zone with nodal temperatures have been analyse using a scanning technique developed in Maple software to determine the position of the ledge profile. To do so, a virtual cylindrical mesh is defined, using a coordinate system locate on the cathode top surface in the middle of the cell (see Figure 5). Considering an appropriate refinement along θ (1°) and z (15 mm), the scanning procedure consists in the computation of the radial location (r_{955}) of the ledge (where temperature reach 955°C) for a given position (θ, z). The scattered data (3D coordinates and temperature) are interpolated using the inverse distance weighted interpolation technique [5] with a spherical influence of 50 mm around the scanned radial position. A typical ledge profile computed using this approach is shown on Figure 6. The comparison between two scenarios is based on a statistical approach using gaussian distribution of the radial gap (Δr) for each position (θ, z) and given by:

$$\Delta r(\theta, z) = r_{955}^{\text{ref}} - r_{955} \tag{1}$$

where:

- r_{955}^{ref} Radial position of the ledge profile for the reference scenario
- r_{955} Radial position of the ledge profile for the scenario under investigation

The sign of Δr indicates a lost (-) or a gain (+) of ledge. The distribution of Δr for a given scenario is validated considering an acceptable confidence interval within a 95 % confidence level.

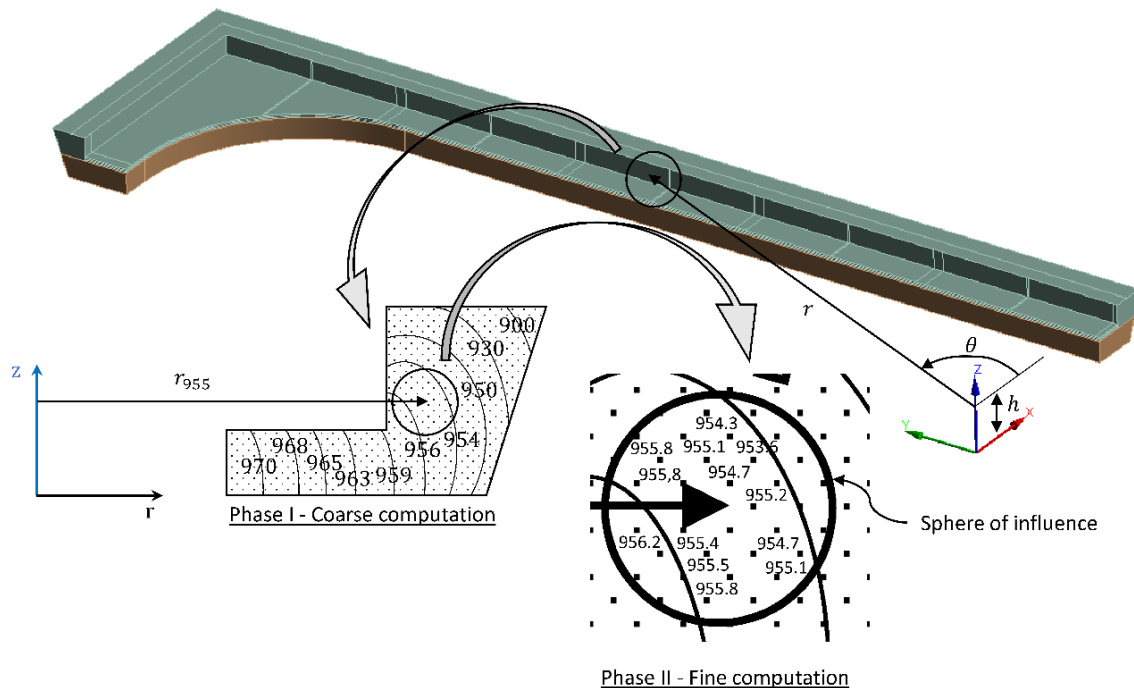


Figure 5. Computation of the ledge profile.

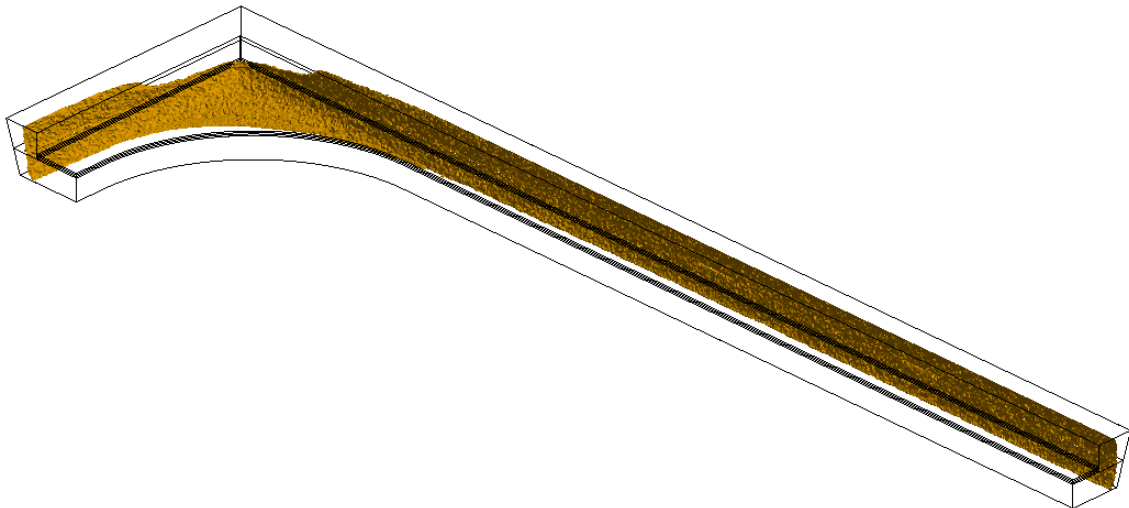


Figure 6. Typical ledge profile from ANSYS™.

6. Results and Interpretation

This section will present the results from the model in order to evaluate the thermoelectrical impact of an additional mass of metal coming from an increase of the metal pad height and the cathode erosion. To simplify reading, the simulated scenarios will be identified using the nomenclature: ‘*Metal height (cm)_Age of cell (years)_Bath Electrical resistivity ($\mu\Omega$ -m)*’.

6.1 Additional Metal Due to Metal Height

To represent a change of the metal pad height, a simple upward translation of the following components was done: liquid bath, fictive material #1, anode assembly and crust (see Figure 2).

Using the computation method explained in section 5, the average ledge thickness of the reference (15_0_4400) was compared to the scenario with 22 cm of metal height. As a reminder, the electrical resistivity of the liquid bath was used to adjust the internal heat in order to fall back on the ledge thickness of the reference. Hence, using a linear interpolation, 3 simulations with 22 cm of metal height were “necessary to estimate the internal heat correction (via the electrical resistivity of the liquid bath) such as:

1. 22_0_4400
2. 22_0_5000
3. 22_0_XXXX

where XXXX is the change in the bath resistivity based on the linear interpolation between scenarios 1 and 2.

Table 3 shows the impact of an additional 7 cm of metal height (from 15 to 22 cm) and Figure 7 shows the ledge profile for each zone of the reduction cell. As shown in the Table 3, considering the hypothesis of the model, adding 7 cm of metal height leads to an increase of the ledge thickness of +28.9 mm if there is no correction of the internal heat. As we can see by the heat loss distribution, this comes mainly from the increased heat loss by the side of the shell considering the higher level of hot liquids.

In Figure 7, by comparing 15_0_4400 and 22_0_4400, the ledge thickness difference of +28.9 mm comes mainly from the short side and the corner of the reduction cell. Also, comparison

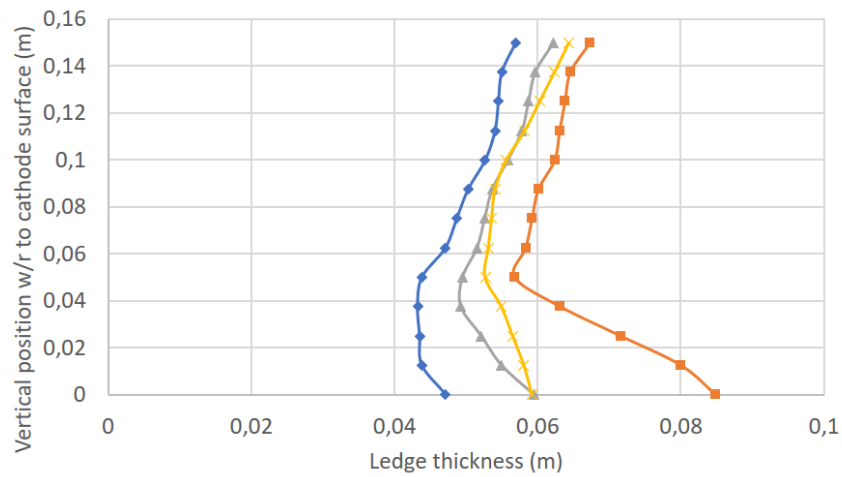
between scenarios 22_0_4400 and 22_0_5000 shows that the ledge thickness is more sensible to the internal heat on the short side and the corner compared to the long side.

For each zone, Figure 7 shows that the highest difference of the ledge thickness occurs at the level of the cathode surface ($y=0$, namely the toe ledge) which can be harmful for the operation since it reduces the available cathode surface for the current. Indeed, by looking at the 955 °C isotherm representing the hot surface of the ledge, Figure 8 shows a significant increase of the covered cathode surface on the short side/corner when operating with an additional 7 cm of metal.

Table 3. Impact of an additional 7 cm of metal height.

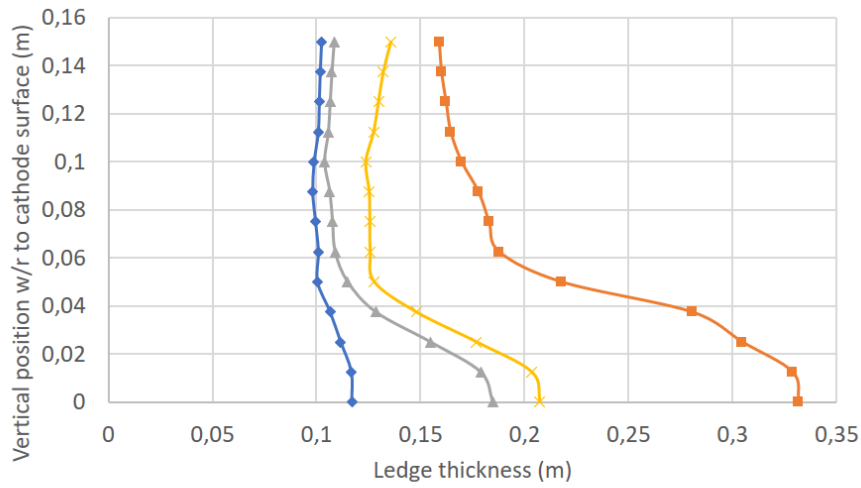
Scenarios	22_0_4400	22_0_5000	22_0_4761
Average ledge thickness [mm]	+28.9	-18.9	-6.9
Confidence interval on ledge calculation [mm]	± 3.4	± 1.8	± 1.1
Average bath temperature under anodes [°C]	-2.9	+0.0	-1.0
Heat loss by the crust and anode assembly [kW]	+1.2	+2.4	+2.0
Heat loss by the side shell [kW]	+2.4	+49.2	+29.7
Heat loss by the bottom shell [kW]	-0.6	+0.3	-0.0
Heat loss by the collector bar [kW]	-0.7	+0.7	+0.2
Heat loss TOT [kW]	+2.2	+52.6	+31.8
Cell voltage [V]	-0.001	+0.155	+0.092

Finally, the linear interpolation base on the average ledge thickness suggests a bath electrical resistivity of 4761 $\mu\Omega\cdot\text{m}$ to represent the amount of internal heat needed to fall back on the reference ledge while having 22 cm of metal height. From Table 3, the linear interpolation leads to a pretty good estimation with a thickness difference of -6.9 mm when compared to the reference (confidence interval of ± 1.1 mm) while using a correction of +92 mV on the cell voltage (+36 kW). Also, Figure 7 shows that 22_0_4761 allows a good match with the ledge thickness for each section on the reduction cell.



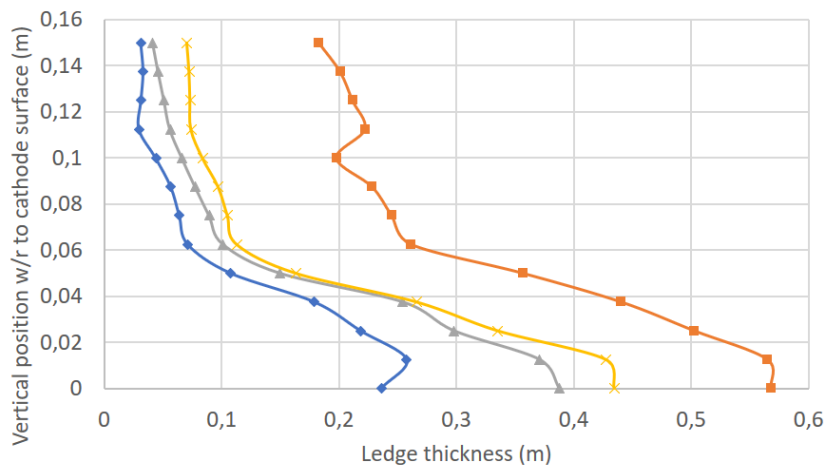
(a)

—■— 22_0_4400 —▲— 22_0_4761 —◆— 22_0_5000 —×— Reference



(b)

—■— 22_0_4400 —▲— 22_0_4761 —◆— 22_0_5000 —×— Reference



(c)

—■— 22_0_4400 —▲— 22_0_4761 —◆— 22_0_5000 —×— Reference

Figure 7. Ledge thickness profile for the scenario with 22 cm of metal height without erosion: long side (a), short side (b), corner (c).

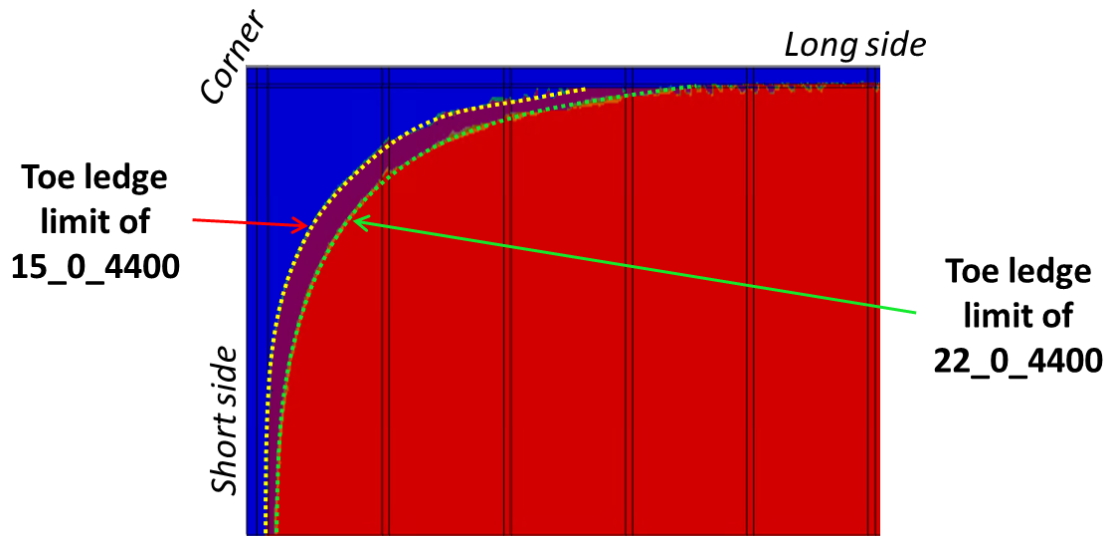
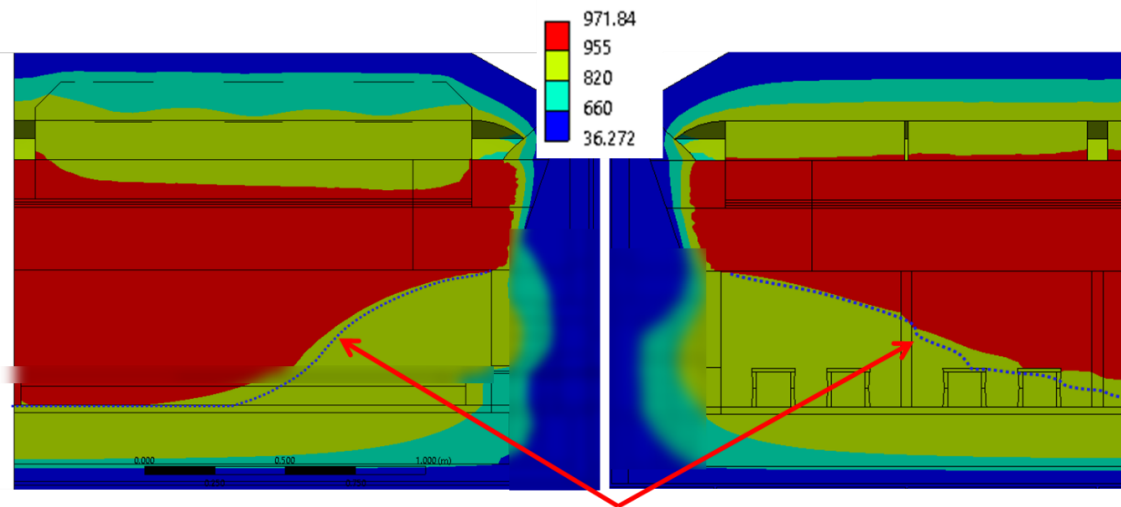


Figure 8. Toe ledge evolution with 7 cm of additional metal height on the first 5 cathodes.

However, since the thermal balance is not the same for 22_0_4761, the critical isotherm may be different from the reference even with a similar ledge profile. Finally, Figure 9 shows that there is only a slight shifting of the 955 °C towards the center on the reduction cell. The others isotherm from the reference are not shown since they are pretty much at the same place.



955 °C isotherm from the reference

(a) (b)
Figure 9. Critical isotherm [°C] of scenario 22_0_4761:
transversal cut (a), longitudinal cut (b).

6.2 Additional Metal Due to Cathode Erosion

The second phenomena leading to an operation with higher mass of metal is due to the cathode erosion through time. To analyse this element, the same strategy as the section 6.1 will be used which lead to compare the reference to 3 new scenarios that include a cathode erosion after 5 years of operation:

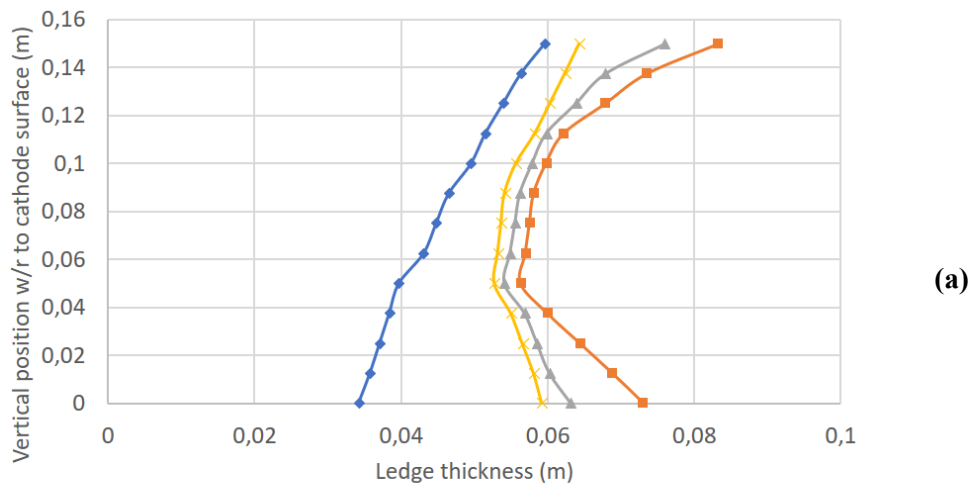
1. 15_5_4400
2. 15_5_5000
3. 15_5_XXXX

Table 4 shows the impact of an additional mass of metal due to 5 years of cathode erosion and Figure 10 shows the ledge profile for each zone of the reduction cell. As shown in the Table 4, considering the hypothesis of the model, a 5 years of cathode erosion leads to an increase of the ledge thickness of only +8.6 mm if there is no correction of the internal heat. As we can see by the heat loss distribution, this comes mainly from the increased heat loss by the bottom of the shell and the collector bar considering the additional metal towards to bottom of the lining replacing the eroded less conductive carbon material.

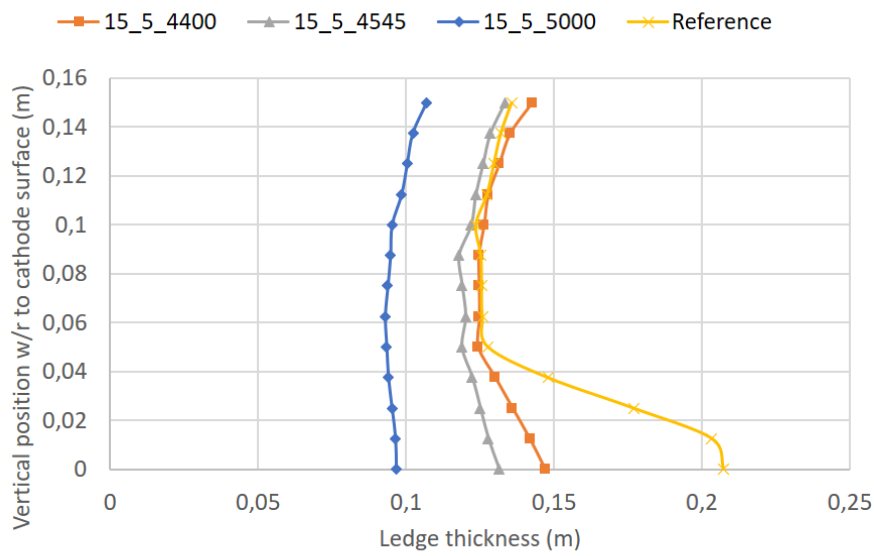
In Figure 10, by comparing 15_0_4400 and 15_5_4400, the ledge thickness difference of +8.6 mm comes mainly from the long side of the reduction cell (unlike the effect of additional metal height). Indeed, as we can see on the short side and the corner, the ledge thickness is almost the same at 50 mm from the cathode surface ($y = 0.05$) and upward. Also, comparison between scenarios 15_5_4400 and 15_5_5000 shows that the ledge thickness is more sensitive to the internal heat on the long side when compared to the short side/corner (unlike the effect of additional metal height). The smaller toe ledge of the eroded scenario ($y = 0$) comes from the fact that the highly conductive metal in the eroded volume brings the 955 °C isotherm slightly towards the bottom on the lining.

Table 4. Impact of additional metal coming from a 5 years cathode erosion.

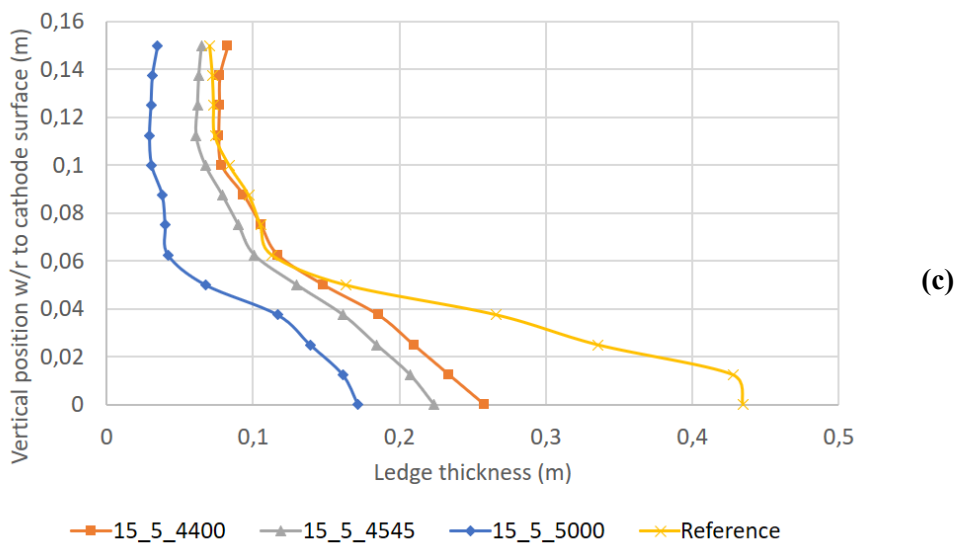
Scenarios	15_5_4400	15_5_5000	15_5_4545
Average ledge thickness [mm]	+8.6	-26.6	+0.1
Confidence interval on ledge calculation [mm]	± 1.8	± 2.5	± 1.9
Average bath temperature under anodes [°C]	-2.5	+0.5	-1.7
Heat loss by the crust and anode assembly [kW]	-0.6	+1.0	-0.2
Heat loss by the side shell [kW]	-0.3	+47.3	+10.7
Heat loss by the bottom shell [kW]	+0.2	+1.1	+0.5
Heat loss by the collector bar [kW]	+0.3	+1.8	+0.7
Heat loss TOT [kW]	-0.3	+51.1	+11.7
Cell voltage [V]	-0.017	+0.139	+0.020



(a)



(b)



(c)

Figure 10. Ledge thickness profile for the scenario with 15 cm of metal height and 5 years of cathode erosion: long side (a), short side (b), corner (c).

This time, the linear interpolation base on the average ledge thickness suggests a bath electrical resistivity of $4545 \mu\Omega\cdot\text{m}$ to represent the amount of internal heat needed to fall back on the reference ledge while having a 5 years erosion profile. From Table 4, the linear interpolation leads to a very good estimation with a thickness difference of $+0.1 \text{ mm}$ when compare to the reference (confidence interval of $\pm 1.9 \text{ mm}$) while using a correction of $+20 \text{ mV}$ on the cell voltage ($+8 \text{ kW}$). Also, Figure 10 shows that 15_5_4545 allows a good match for each section.

Figure 11 shows that the 15_5_4545 scenario leads to a slight shifting of the $955 \text{ }^\circ\text{C}$ isotherm towards the lining which lead to an increase of $5 \text{ }^\circ\text{C}$ of the collector bars (average of the sealed zone). However, there is this no significative changes for the $820\text{--}660 \text{ }^\circ\text{C}$ isotherms.

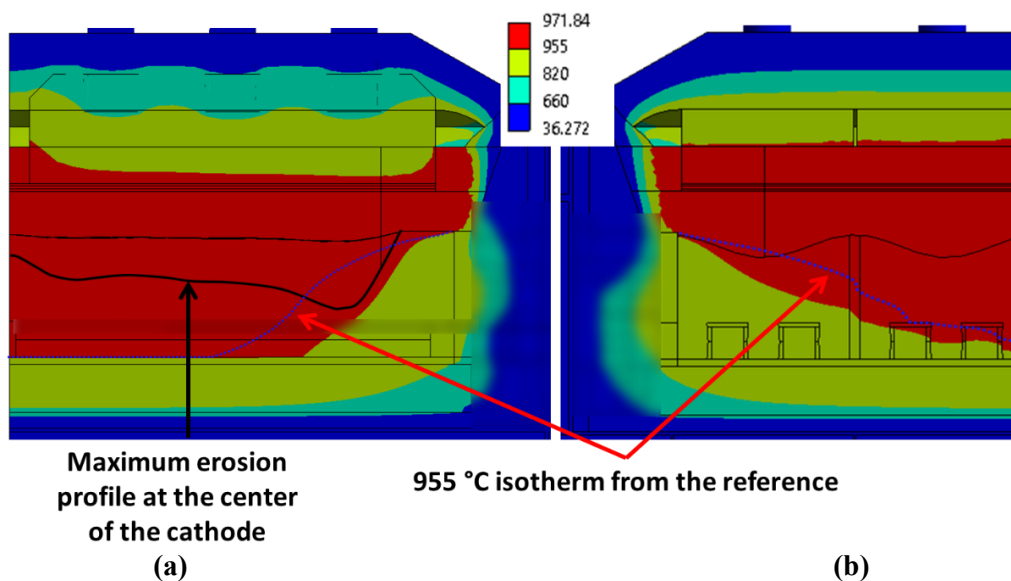


Figure 11. Critical isotherm [$^\circ\text{C}$] of scenario 15_5_4545: transversal cut (a), longitudinal cut (b).

Unlike the metal pad height, the cathode erosion leads to a significative change in the current density distribution in the metal pad and the cathode plane. Figure 12 shows that the shorter/less resistive path created by the erosion profile leads to the concentration of the current lines at the maximum erosion point. As shown in Figure 13 (a) and (b), the erosion causes a less uniform current density distribution in the metal pad/cathode plane when compared to the reference scenario which may lead to significative changes in the MHD behaviour of the reduction cell.

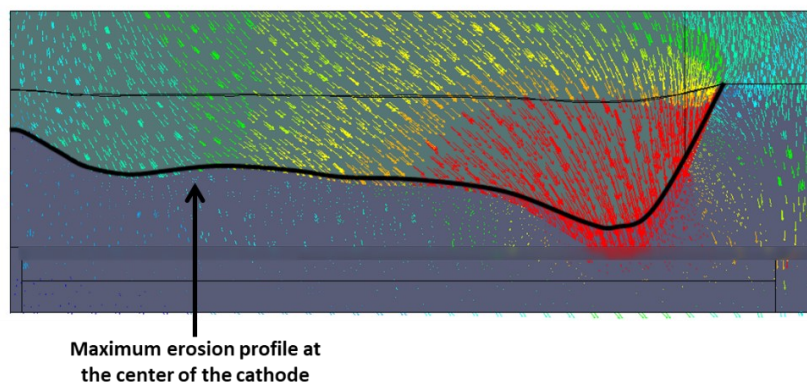


Figure 12. Impact of the erosion on the current density vectors.

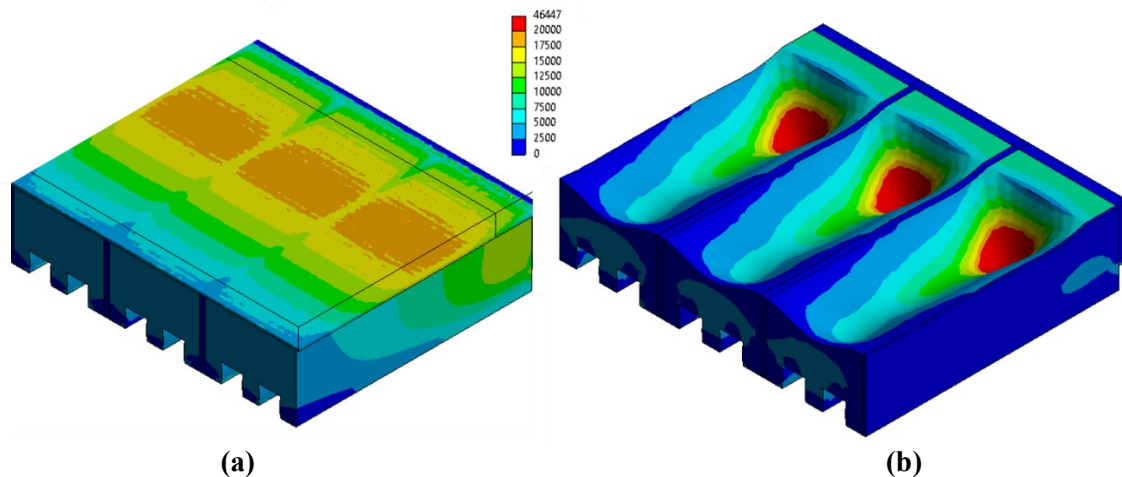


Figure 13. Impact of the erosion on the current density [A/m²]: current density of the reference (a), current density after 5 years of erosion (b).

7. Conclusion

This paper describes the development of a quarter cell model to study the impact of an additional mass of metal in a reduction cell. To do so, a transient thermoelectrical analysis was used with a bi-phasic material in order to take into account the position of the solid ledge according to the thermal and electrical behaviour of the reduction cell.

The model predicted a resulting ledge profile for each one of the investigated scenarios which were quantitatively compared to the reference scenario using an external calculation procedure.

The results associated to an additional metal pad height allow to estimate a cell voltage correction of +92 mV (+36 kW) in order to fall back on the reference ledge. This internal energy change leads to only a slight shifting of the 955 °C isotherm towards the centre on the reduction cell.

As for the results associated to an additional metal mass via the erosion of the cathode, the model estimates a cell voltage correction of +20 mV (+8 kW) in order to fall back on the reference ledge. This internal energy change leads to a slight shifting of the 955 °C isotherm towards the lining which lead to an increase of 5 °C of the collector bars.

Note that the model doesn't consider the changes in the thermodynamic of the bath following a variation of the thermal balance. Nevertheless, this study may help to orientate some applicable decisions regarding the operation or the conception.

Finally, the erosion causes important variations of the density distribution in the metal pad/cathode plane which may lead to significative changes in the MHD behaviour of the reduction cell. It would be constructive to evaluate this impact to find corrective measures in order to keep an optimal operation towards the cell live.

8. Acknowledgments

The authors acknowledge the Aluminum Research Center – REGAL and Aluminerie Alouette Inc. for their financial support as well as the latter for their invaluable contribution to this work.

9. References

1. Simon-Olivier Tremblay, D. Marceau et al. Numerical Investigation of Thermal, Electrical and Mechanical Behaviour of Aluminium Cell During Preheating Phase, *Light Metals* 2023, 765-772.
2. Simon-Olivier Tremblay, D. Marceau et al. In Situ Investigation of the Behavior of Anode Assemblies, *Light Metals* 2016, 959-964.
3. Marc Dupuis and Alton Tabereaux, Modeling Cathode Cooling Due to Power Interruption, *Light Metals* 2012, 923-928.
4. Teklu Hadgu and al., Comparison of CFD Natural Convection and Conduction-Only Models for Heat Transfer in the Yucca Mountain Drifts, *ASME 2004 Heat Transfer/Fluids Engineering Summer Conference*, 223-232.
5. Richard Franke, Scattered data Interpolation: Tests of some methods, *Mathematics of Computation*, vol. 38, 1982, 181–200.